

## Synthesis and Characterization of Carboxylate-Rich Complexes Having the $\{\text{Fe}_2(\mu\text{-OH})_2(\mu\text{-O}_2\text{CR})\}^{3+}$ and $\{\text{Fe}_2(\mu\text{-O})(\mu\text{-O}_2\text{CR})\}^{3+}$ Cores of $\text{O}_2$ -Dependent Diiron Enzymes

Sungho Yoon and Stephen J. Lippard\*

Department of Chemistry, Massachusetts Institute of Technology, Cambridge, Massachusetts 02139

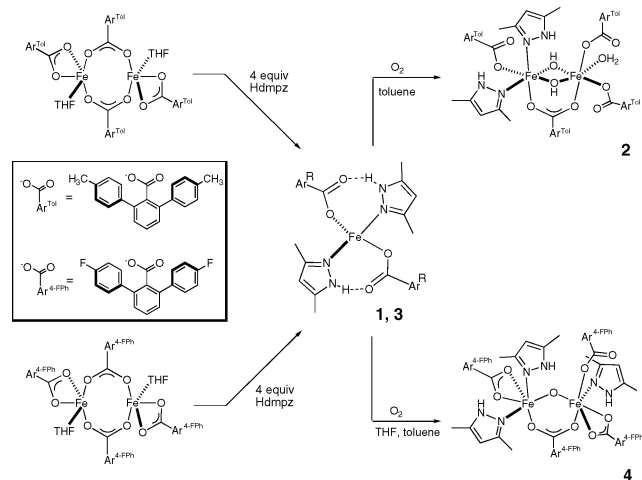
Received December 9, 2003; E-mail: lippard@lippard.mit.edu

Carboxylate-bridged diiron centers activate dioxygen for radical generation and hydrocarbon oxidation at the active sites of enzymes such as class I ribonucleotide reductase (RNR-R2), soluble methane monooxygenase hydroxylase (sMMOH), and  $\Delta^9$  desaturase ( $\Delta^9\text{D}$ ).<sup>1–3</sup> The dimetallic cores in these enzymes are coordinated by four carboxylate and two imidazole ligands derived from amino acid residues housed in four-helix bundles.<sup>4–7</sup> This structural motif is effectively utilized to achieve diverse physiological functions in these and related proteins.<sup>8</sup> To understand the chemistry of these enzymes at the molecular level, much effort has been expended to reproduce their active-site architecture and reactivity in synthetic models. The  $\{\text{Fe}_2(\mu\text{-OH})_2(\mu\text{-O}_2\text{CR})\}^{3+}$  and  $\{\text{Fe}_2(\mu\text{-O})(\mu\text{-O}_2\text{CR})\}^{3+}$  cores at the active sites of many of these enzymes have been unexpectedly difficult to reproduce in a carboxylate-rich metal coordination environment, however, because of the propensity of iron(III) salts to form oligo- or polynuclear complexes.<sup>9</sup> As a consequence, our current understanding of the physical properties of these diiron units has had to rely upon comparisons with model complexes in N-rich metal coordination environments.<sup>10</sup> In this communication, we report that direct oxygenation of mononuclear iron(II) complexes generates carboxylate-rich compounds encapsulating the desired  $\{\text{Fe}_2(\mu\text{-OH})_2(\mu\text{-O}_2\text{CR})\}^{3+}$  and  $\{\text{Fe}_2(\mu\text{-O})(\mu\text{-O}_2\text{CR})\}^{3+}$  cores with geometries structurally similar to that of the diiron(III) sites in oxidized MMOH and RNR-R2, respectively. In addition to structural resemblance, these diiron(III) complexes share several key physical properties with the enzymes, including Mössbauer spectral and magnetic exchange coupling parameters.

Sterically hindered terphenyl-derived benzoate analogues provide a ligand framework that facilitates assembly of both mononuclear and dinuclear iron complexes.<sup>11–13</sup> Reaction of  $[\text{Fe}_2(\mu\text{-O}_2\text{CAr}^{\text{Tot}})_2(\text{O}_2\text{CAr}^{\text{Tot}})_2(\text{THF})_2]$ , where  $^-\text{O}_2\text{CAr}^{\text{Tot}}$  is 2,6-di(*p*-tolyl)benzoate, with 4 equiv of 3,5-dimethylpyrazole (Hdmpz) yielded the mononuclear iron(II) complex,  $[\text{Fe}(\text{O}_2\text{CAr}^{\text{Tot}})_2(\text{Hdmpz})_2]$  (**1**) (Scheme 1 and Supporting Information). Compound **1** has a pseudo-tetrahedral iron(II) center bound to two monodentate carboxylates and two Hdmpz ligands (Figure S1). Two hydrogen-bonding interactions occur between the  $\text{Ar}^{\text{Tot}}\text{CO}_2^-$  and Hdmpz ligands, as revealed by  $\text{O}\cdots\text{H}\cdots\text{N}$  distances of 2.743(2) and 2.783(2) Å. The combined influence of these intramolecular hydrogenbonding interactions with sterically hindered carboxylate ligands stabilizes **1** with an uncommonly low coordination number of 4 for a  $[\text{M}(\text{O}_2\text{CR})_2\text{L}_2]$  complex.

Exposure of a colorless toluene solution of **1** to dioxygen at room temperature rapidly afforded the yellow diiron(III) complex,  $[\text{Fe}_2(\mu\text{-OH})_2(\mu\text{-O}_2\text{CAr}^{\text{Tot}})(\text{O}_2\text{CAr}^{\text{Tot}})_3(\text{OH}_2)(\text{Hdmpz})_2]$  (**2**) (Figures 1 and S2), in 70% yield. The two iron atoms have pseudo-octahedral coordination and are bridged by one carboxylate and two hydroxo ligands. The  $\text{Fe}\cdots\text{Fe}$  distance of 2.996(2) Å is similar to those previously reported for di( $\mu$ -hydroxo)( $\mu$ -carboxylato)diiron(III) cores: 2.99–3.14 and 2.9788(6) Å for resting state sMMOH<sub>ox</sub><sup>5,14</sup> and the  $[\text{Fe}_2(\mu\text{-OH})_2(\mu\text{-O}_2\text{CAr}^{\text{Tot}})(\text{O}_2\text{CAr}^{\text{Tot}})_3(\text{Bn}_2\text{en})(\text{Bnen})]$  com-

Scheme 1



plex,<sup>15,16</sup> respectively. The latter compound is the only other known synthetic analogue of oxidized MMOH having the  $\{\text{Fe}_2(\mu\text{-OH})_2(\mu\text{-O}_2\text{CR})\}^{3+}$  core. In addition to bridging ligands, the coordination sphere of Fe1 includes one monodentate carboxylate and two Hdmpz ligands to complete an N<sub>2</sub>O<sub>4</sub> donor atom set. For Fe2, an O<sub>6</sub> set of donor atoms arises by addition of two monodentate terminal carboxylates and a water molecule.

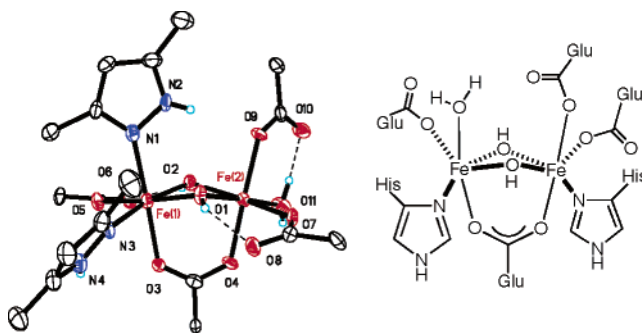


**Figure 1.** Left: ORTEP diagram with 50% probability thermal ellipsoids;  $[\text{Fe}_2(\mu\text{-OH})_2(\mu\text{-O}_2\text{CAr}^{\text{Tot}})(\text{O}_2\text{CAr}^{\text{Tot}})_3(\text{OH}_2)(\text{Hdmpz})_2]$  (**2**). The phenyl rings of  $\text{Ar}^{\text{Tot}}\text{CO}_2^-$  ligands are omitted for clarity. Selected interatomic distances (Å) and angles (deg): Fe1⋯Fe2, 2.996(2); Fe1–O1, 1.953(5); Fe1–O2, 1.958(5); Fe2–O1, 1.944(5); Fe2–O2, 2.012(5); O1⋯O8, 2.627(8); O2⋯O6, 2.801(7); O10⋯O11, 2.506(9); Fe1–O1–Fe2, 100.3(3); Fe1–O2–Fe2, 98.1(2). Right: The structure of the diiron core in the MMOH<sub>ox</sub> resting state.

The terminal carboxylates are each hydrogen-bonded to a bridging hydroxo or the water ligand. Interactions of this kind occur in MMOH<sub>ox</sub><sup>5,14</sup> and may be required for stability of the  $\{\text{Fe}_2(\mu\text{-OH})_2(\mu\text{-O}_2\text{CR})\}^{3+}$  core. The two iron sites in **2** are asymmetric, and the molecule crystallizes as a racemate.

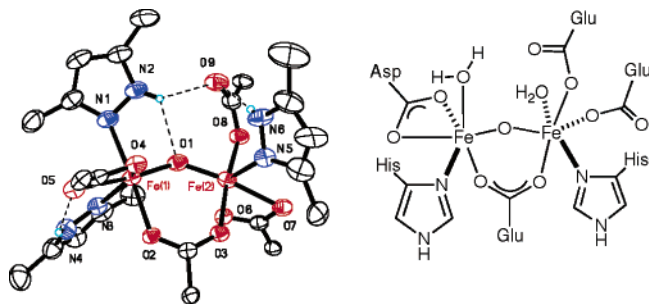


**Figure 2.** Left: ORTEP diagram with 50% probability thermal ellipsoids;  $[\text{Fe}_2(\mu\text{-O})(\mu\text{-O}_2\text{CAR}^{4\text{-FPh}})(\text{O}_2\text{CAR}^{4\text{-FPh}})_3(\text{Hdmpz})_3]$  (**4**). The phenyl rings of  $\text{Ar}^{\text{Tot}}\text{CO}_2^-$  ligands are omitted for clarity. Selected interatomic distances (Å) and angles (deg):  $\text{Fe1}\cdots\text{Fe2}$ , 3.3429(9);  $\text{Fe1-O1}$ , 1.772(3);  $\text{Fe2-O1}$ , 1.786(3);  $\text{O1}\cdots\text{N2}$ , 2.821(5);  $\text{O5}\cdots\text{N4}$ , 2.780(5);  $\text{N6}\cdots\text{O9}$ , 2.885(6);  $\text{N2}\cdots\text{O9}$ , 2.857(6);  $\text{Fe1-O1-Fe2}$ , 139.94(14). The phenyl rings of  $\text{Ar}^{4\text{-FPh}}\text{CO}_2^-$  ligands are omitted for clarity. Right: The structure of the diiron core in the RNR-R2<sub>act</sub> resting state.

The 4.2 K zero-field Mössbauer spectrum of solid **2** exhibits a quadrupole doublet with  $\delta = 0.45$  (2) mm/s,  $\Delta E_Q = 1.21$  (2) mm/s, and  $\Gamma = 0.36$  (2) mm/s (Figure S3), indicating indistinguishable iron(III) atoms. The isomer shift ( $\delta$ ) falls in the range typical of the high-spin Fe(III) complexes.<sup>10</sup> The quadrupole splitting parameter ( $\Delta E_Q$ ) unexpectedly differs from that of the structurally related  $[\text{Fe}_2(\mu\text{-OH})_2(\mu\text{-O}_2\text{CAR}^{\text{Tot}})(\text{O}_2\text{CAR}^{\text{Tot}})_3(\text{Bn}_2\text{en})(\text{Bnen})]$  complex ( $\Delta E_Q = 0.61$  (2) mm/s).<sup>15,16</sup> Considering that most of the reported hydroxo-bridged diiron(III) complexes have  $\Delta E_Q$  values  $\sim 0.5$  mm/s,<sup>10</sup> **2** is unique among synthetic models but more closely resembles the diiron core in sMMOH<sub>ox</sub> ( $\Delta E_Q = 0.87$  and 1.16 mm/s).<sup>17</sup> This result most likely reflects the fact that **2** is the first complex to match the O-rich environment in the enzyme and is unique in having the terminally bound water molecule observed in all forms of sMMOH structurally characterized to date.<sup>5,14</sup> The similarities in the geometric and Mössbauer spectral properties of the diiron(III) centers in sMMOH and **2** led us to measure its temperature-dependent magnetic susceptibility (Figure S4). Analysis of the data revealed a spin exchange coupling constant  $J$  of  $-7.2$  (2)  $\text{cm}^{-1}$  with  $g$  fixed as 2.0 ( $H = -2J\mathbf{S}_1\cdot\mathbf{S}_2$ , where  $S_1 = S_2 = 5/2$ ). This weak antiferromagnetic behavior is identical to that in sMMOH<sub>ox</sub>, for which  $J$  is also  $-7$  (3)  $\text{cm}^{-1}$ ,<sup>17</sup> consistent with the close similarities in their other physical properties.

The mononuclear complex  $[\text{Fe}(\text{O}_2\text{CAR}^{4\text{-FPh}})_2(\text{Hdmpz})_2]$  (**3**) (Figure S5), where  $^-\text{O}_2\text{CAR}^{4\text{-FPh}}$  is 2,6-di(*p*-fluorophenyl)-benzoate, an analogue of **1**, was prepared in a similar manner from  $[\text{Fe}_2(\mu\text{-O}_2\text{CAR}^{4\text{-FPh}})_2(\text{O}_2\text{CAR}^{4\text{-FPh}})_2(\text{THF})_2]$ . Oxygenation of a THF or toluene solution of **3** afforded the brown diiron(III) complex,  $[\text{Fe}_2(\mu\text{-O})(\mu\text{-O}_2\text{CAR}^{4\text{-FPh}})(\text{O}_2\text{CAR}^{4\text{-FPh}})_3(\text{Hdmpz})_3]$  (**4**) (Figures 2 and S6) in 78% yield. The two asymmetric iron atoms have a distorted octahedral geometry and are linked by only one carboxylate and one oxo group. The  $\text{Fe}\cdots\text{Fe}$  distance (3.3429(9) Å) of **4** is similar to the 3.3–3.4 Å found in the  $(\mu\text{-oxo})(\mu\text{-carboxylato})$ diiron(III) core of RNR-R2<sup>4</sup> and slightly longer than those of reported  $\{\text{Fe}_2(\mu\text{-O})(\mu\text{-O}_2\text{CR})\}^{3+}$  complexes with N-rich coordination environments.<sup>18–20</sup> The remaining coordination sites of **4** are completed by three Hdmpz and three carboxylate ligands, again generating carboxylate-

rich metal coordination environments for the two iron atoms. The 4.2 K Mössbauer spectrum of **2** exhibits a quadrupole doublet with  $\delta = 0.51$  (2) mm/s,  $\Delta E_Q = 1.26$  (2) mm/s, and  $\Gamma = 0.30$  (2) mm/s (Figure S7). The small  $\Delta E_Q$  value is at the lower end of the range ( $> 1$  mm/s) for most oxo-bridged diiron(III) complexes. The strong antiferromagnetic exchange coupling,  $J = -117.2$  (1)  $\text{cm}^{-1}$ , in **4** (Figure S8) compares favorably with that of RNR-R2, where  $J$  is  $-110$   $\text{cm}^{-1}$ , and is typical for other reported  $(\mu\text{-oxo})(\mu\text{-carboxylato})$  diiron(III) complexes ( $J = -90$  to  $-120$   $\text{cm}^{-1}$ ).<sup>10</sup>

In summary, this work provides efficient syntheses, by direct oxygenation of the mononuclear iron(II) precursors, of diiron(III) complexes containing the biomimetic  $\{\text{Fe}_2(\mu\text{-OH})_2(\mu\text{-O}_2\text{CR})\}^{3+}$  and  $\{\text{Fe}_2(\mu\text{-O})(\mu\text{-O}_2\text{CR})\}^{3+}$  cores present in carboxylate-bridged diiron enzymes. Key physical properties of the enzyme active sites were successfully reproduced by these small molecules, which mimic both the bridging modes and the O-rich environments. Possible intermediate(s) and mechanistic details involved in the oxygenation pathway are currently under investigation.

**Acknowledgment.** This work was supported by Grant GM32134 from the National Institute of General Medical Sciences. We thank Dr. J. Kuzelka for assistance in acquiring the Mössbauer spectra and Dr. L. Beauvais for helpful discussions.

**Supporting Information Available:** Details of the synthetic procedures, physical characterization of **2** and **4**, and ORTEP diagrams including all non-hydrogen atoms of compounds **1–4** (PDF). X-ray crystallographic files for these compounds (CIF). This material is available free of charge via the Internet at <http://pubs.acs.org>.

## References

- Solomon, E. I.; Brunold, T. C.; Davis, M. I.; Kemsley, J. N.; Lee, S.-K.; Lehnert, N.; Neese, F.; Skulan, A. J.; Yang, Y.-S.; Zhou, J. *Chem. Rev.* **2000**, *100*, 235–349.
- Waller, B. J.; Lipscomb, J. D. *Chem. Rev.* **1996**, *96*, 2625–2657.
- Merkx, M.; Kopp, D. A.; Sazinsky, M. H.; Blazyk, J. L.; Müller, J.; Lippard, S. J. *Angew. Chem., Int. Ed.* **2001**, *40*, 2782–2807.
- Nordlund, P.; Eklund, H. J. *Mol. Biol.* **1993**, *232*, 123–164.
- Whittington, D. A.; Lippard, S. J. *J. Am. Chem. Soc.* **2001**, *123*, 827–838.
- Rosenzweig, A. C.; Frederick, C. A.; Lippard, S. J.; Nordlund, P. *Nature* **1993**, *366*, 537–543.
- Lindqvist, Y.; Huang, W.; Schneider, G.; Shanklin, J. *EMBO J.* **1996**, *15*, 4081–4092.
- Du Bois, J.; Mizoguchi, T. J.; Lippard, S. J. *Coord. Chem. Rev.* **2000**, *200–202*, 443–485 and references cited therein.
- Lippard, S. J. *Angew. Chem., Int. Ed. Engl.* **1988**, *27*, 344–361.
- Kurtz, D. M., Jr. *Chem. Rev.* **1990**, *90*, 585–606 and references cited therein.
- Lee, D.; Lippard, S. J. *Inorg. Chem.* **2002**, *41*, 2704–2719.
- Lee, D.; Lippard, S. J. *Inorg. Chim. Acta* **2002**, *341*, 1–11.
- Hagadorn, J. R.; Que, L., Jr.; Tolman, W. B. *Inorg. Chem.* **2000**, *39*, 6086–6090.
- Elango, N.; Radhakrishnan, R.; Froland, W. A.; Waller, B. J.; Earhart, C. A.; Lipscomb, J. D.; Ohlendorf, D. H. *Protein Sci.* **1997**, *6*, 556–568.
- Lee, D.; Lippard, S. J. *Inorg. Chem.* **2002**, *41*, 827–837.
- Lee, D.; Lippard, S. J. *J. Am. Chem. Soc.* **2001**, *123*, 4611–4612.
- Fox, B. G.; Hendrich, M. P.; Surerus, K. K.; Andersson, K. K.; Froland, W. A.; Lipscomb, J. D.; Münck, E. *J. Am. Chem. Soc.* **1993**, *115*, 3688–3701.
- Marlin, D. S.; Olmstead, M. M.; Mascharak, P. K. *Inorg. Chem.* **2003**, *42*, 1681–1687.
- Yan, S.; Que, L., Jr. *J. Am. Chem. Soc.* **1988**, *110*, 5222–5224.
- Yan, S.; Cox, D. D.; Pearce, L. L.; Juarez-Garcia, C.; Que, L., Jr.; Zhang, J. H.; O'Connor, C. J. *Inorg. Chem.* **1989**, *28*, 2507–2509.

JA031603O